Green Chemistry

ROYAL SOCIETY OF CHEMISTRY

CRITICAL REVIEW

View Article Online
View Journal | View Issue

Cite this: *Green Chem.*, 2024, **26**, 8052

Catalytic production of 1,4-pentanediol from lignocellulosic biomass

Shanhui Zhu, *[a,b] Zexiang Lv,[a,b] Jiamin Wang,[a,b] Xiangyu Jia,[a,b] Xiaoming Li,[a,b] Mei Dong,[a] Jianguo Wang *[b] and Weibin Fan *[a]

Received 12th January 2024,
Accepted 7th March 2024

DOI: 10.1039/d4gc00180j

rsc.li/greenchem

Sustainable production of 1,4-pentanediol (1,4-PDO) from biomass is of great importance because 1,4-PDO is a monomer of degradable polyesters and plastics. This paper reviews the conversion of biomass-derived levulinic acid (LA) and furfural as well as their derivatives alkyl levulinate, γ-valerolactone (GVL) and furfuryl alcohol (FAL) into 1,4-PDO. MoO_x or ReO_x modified noble metal catalysts and non-noble metal catalysts with core–shell and alloy structures show a high 1,4-PDO yield and stability in LA hydrogenation under severe hydrothermal conditions. The conversion of furfural to 1,4-PDO involves the initial C=O bond hydrogenation to form FAL, the consecutive acid-catalyzed ring-opening and the final hydrogenation. Therefore, it needs a bifunctional catalyst composed of metallic species and acid sites to improve the 1,4-PDO yield. Efforts are made here to highlight the employed catalysts, structure–performance relationship, reaction pathway and reaction mechanism in detail. The current challenges for large-scale applications of conversion of LA and furfural to 1,4-PDO have been proposed, including process development, catalyst cost, solvent and active site distribution. We believe that this review will provide new opportunities and expand the options for the production of 1,4-PDO *via* biorefining processes.

1. Introduction

Conversion of huge amounts of biomass into fuels and chemicals is a potentially effective strategy for achieving carbon neutrality and is a great challenge.[1–6] Non-edible and renewable lignocellulose consists of cellulose, hemicellulose and lignin.[7] It accounts for more than 95% of biomass resources that are annually produced, about 170 billion tons.[7] Although it is

[a]*State Key Laboratory of Coal Conversion, Institute of Coal Chemistry, Chinese Academy of Sciences, Taiyuan 030001, PR China. E-mail: zhushanhui@sxicc.ac.cn, fanwb@sxicc.ac.cn*
[b]*University of Chinese Academy of Sciences, Beijing 100049, PR China. E-mail: iccjgw@sxicc.ac.cn*

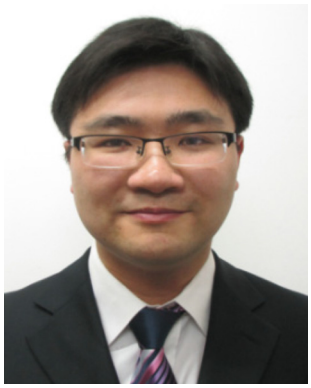

Shanhui Zhu

Shanhui Zhu obtained his Ph.D. degree in 2014 from the Institute of Coal Chemistry at the Chinese Academy of Sciences (ICCCAS) under the supervision of Prof. Yulei Zhu with the research topic of catalytic hydrogenolysis of glycerol to value-added chemicals. Right now, he is working as a professor at ICCCAS. His current research interests are biomass conversion and heterogeneous catalysis.

Jiamin Wang

Jianguo Wang is currently a professor and has been the Vice Director of Chemical Engineering College in the University of Chinese Academy of Sciences since 2019. He was born in 1962 and received his Ph.D. degree in 1995. In 1996, he worked with the aid of an Alexander von Humboldt fellowship in the University of Erlangen-Nuremberg, Germany. He worked in ICCCAS after 1998 with the financial support by the "Hundred Talents Project" of CAS in 2000. His research mainly includes coal chemistry, heterogeneous catalysis and zeolites. He has published more than 300 peer-reviewed papers.

highly significant to valorize sustainable production of chemicals and biofuels from lignocellulose, technological advances are important and necessary. Reductive catalytic fractionation, known as the lignin first strategy, involves lignocellulose solvolysis, extraction and stabilization of reactive lignin fragments and subsequent conversion, which has been demonstrated to be powerful technology with potential to increase the profitability and sustainability of future biorefineries.[4,5] Sels *et al.*[5] successfully converted birch wood into high value-added phenol, propylene, oligomers and pulp using this approach. Barta *et al.*[6] sought an effective deep eutectic solvent composed of choline chloride, oxalic acid and ethylene glycol for lignocellulose fractionation, in which the obtained lignin with a high β-O-4 content can be efficiently converted into distinct monophenolic compounds, while the cellulose residues were readily depolymerized to 95.9% glucose yield through enzymatic catalysis. Besides, a variety of catalytic methods and innovative biorefinery approaches have been developed to produce various platform chemicals, such as furfural,[8,9] levulinic acid (LA),[10,11] 5-hydroxymethylfurfural,[12,13] glycerol,[14] guaiacol[15] and so on. These platform chemicals can be further converted into many types of value-added products through hydrogenation, oxidation, esterification and even complex cascade processes.

1,4-Pentanediol (1,4-PDO), like other bio-diols, is a building block of degradable polyesters and plastics.[16,17] 1,4-PDO can integrate with long-chain diacids (>C_{12}) to produce crystalline polyesters that are amenable to develop shape-memory polymers due to their low switching temperature (<0 °C).[18] This unique thermosensitive adhesive can hold wide potential applications in the packaging of temperature-sensitive goods, adhesives, coatings, and elastomeric/rubbery materials. Besides, 1,4-PDO is widely used as an industrial solvent. Currently, 1,4-PDO is commercially produced by the condensation of hydroquinone and acetic anhydride over homogeneous NaOH or H_2SO_4 catalysts. The total European and USA production was 18 000 tons and its market price can reach $3000 per ton.[19]

Weibin Fan

Weibin Fan earned his Ph.D. degree from ICCCAS in 1998. From 1999 to 2001, he conducted a postdoctoral fellowship with Prof. Robert A. Schoonheydt and Bert M. Weckhuysen at the Catholic University of Leuven, Belgium. After that, he continued to conduct a postdoctoral fellowship under Prof. Takashi Tatsumi with financial aid from the Japan Society for Promotion of Science (JSPS) and the Japan Agency of Science and Technology (JST). Since 2007, he has been employed in ICC and has been working as a full professor. His research interests focus on zeolites, heterogeneous catalysis and biomass conversion.

Currently, optically active 2,4-pentanediol has been employed as a chiral linking bridge to synthesize enantiomerically pure reagents, such as binaphthol and 2-hydroxycyclohexanone acetal.[20,21] 1,4-PDO has one asymmetric carbon and a similar structure to 2,4-pentanediol. Thus, the greener 1,4-PDO holds the potential to substitute 2,4-pentanediol as a highly efficient and widely applicable stereocontroller in the future. Obviously, it is urgent and necessary to develop the production process of optically pure 1,4-PDO.

In light of the heavy pollution from the conventional petroleum route, two platform chemicals, *i.e.* cellulose-derived LA and hemicellulose-derived furfural, have been employed to produce 1,4-PDO from renewable biomass. As shown in Scheme 1, LA is sequentially hydrogenated into 1,4-PDO. In alcohol solvent, alkyl levulinate is formed by LA esterification. It can be hydrogenated to γ-valerolactone (GVL) that is further converted into 1,4-PDO through consecutive hydrogenation. Conversion of furfural to 1,4-PDO is achieved through consecutive hydrogenations and a ring-opening reaction with the formed FAL alcoholysis to alkyl levulinate that is converted to 1,4-PDO *via* GVL. This shows that one route for the production of 1,4-PDO is from LA and its derivatives of alkyl levulinate and GVL as feedstocks, and the other route involves the use of furfural and its derivatives FAL, 2-methylfuran (2-MF) and 2-methyltetrahydrofuran (2-MTHF) as starting materials. The two routes require heterogeneous catalysts with different types of active sites.[22–24]

The employed catalyst systems, structure–performance relationship, reaction pathway and catalytic mechanism are reviewed here in detail, and the challenges for large-scale production of 1,4-PDO are described, including reactors, catalyst cost, solvent and active site distribution. In addition, the future prospects and mechanic investigation for rational and precise catalyst design are envisaged by using Earth-abundant metals and developing more benign yet competitive catalysts.

2. Conversion of LA and its derivatives into 1,4-PDO

2.1. Conversion of LA into 1,4-PDO

2.1.1. Noble metal catalysts for conversion of LA into 1,4-PDO. In comparison with Pt-group metals, Ru is surprisingly active in the aqueous-phase hydrogenation of LA, because the high oxophilicity of Ru (d-band center) facilitates the adsorption of the C=O bond of LA.[25] Thus, Ru-based catalysts are mostly used for conversion of biomass-based LA, particularly with water as the solvent.[26–29] Many research results have demonstrated that water adsorbed on the Ru site generates a proton, which can participate in the LA hydrogenation.[30,31] The nanoporous metal possesses a high surface-to-volume ratio and abundant low-coordinated surface sites, and thus, shows excellent performance. Lv *et al.*[32] developed a highly active and selective nanoporous Ru catalyst, which gave a 1,4-PDO yield of 78.8% at 100 °C in water solvent (entry 1, Table 1). The suitable acid sites and lattice planes of this cata-

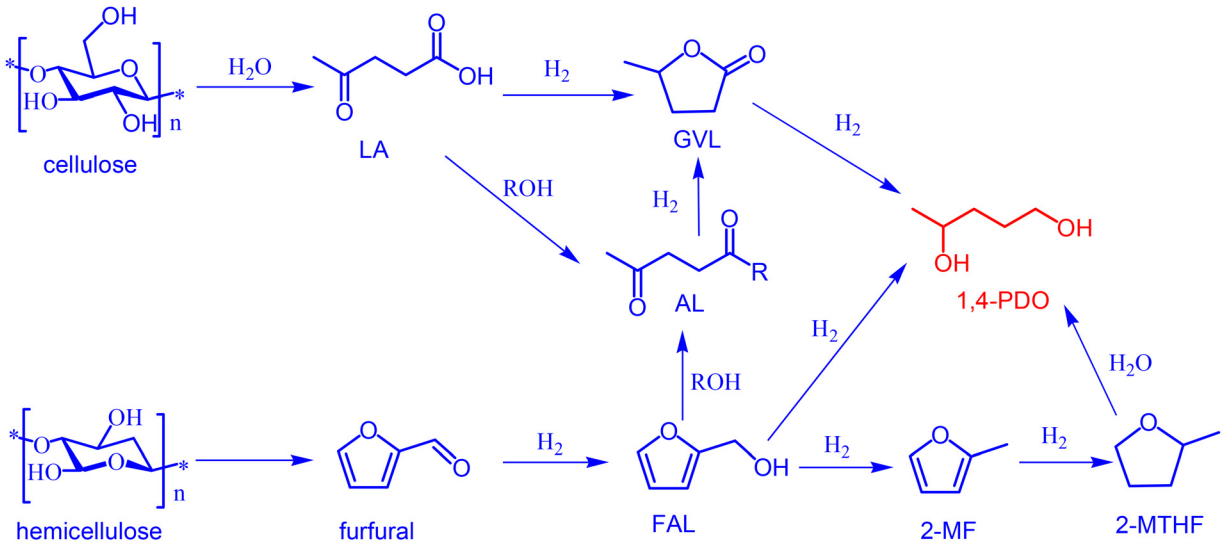

Scheme 1 Reaction pathways for the production of 1,4-PDO from cellulose and hemicellulose derivatives. AL: alkyl levulinate.

Table 1 Comparison of the catalytic performances of LA hydrogenation to 1,4-PDO over representative catalysts

Entry	Catalyst	Temperature (°C)	H_2 pressure (MPa)	Solvent	Conv. (%)	1,4-PDO Yield (%)	Ref.
1	Nanoporous Ru	100	6	H_2O	100	78.8	32
2	RuRe/C	140	15	H_2O	100	82	37
3	Rh–MoO_x/SiO_2	80	6	H_2O	100	70	38
4	Ru–MoO_x/AC	70	4	H_2O	99.9	96.7	39
5	Ru–MoO_x/TiO_2	110	4	H_2O	100	91	40
6	Pt–MoO_x/HAP	130	5	H_2O	>99	93	41
7	Pd_n/NC@SBA-15	80	0.1	Ethanol	>99	>99	47
8	Au/TiO_2	200	5	Free	100	100	49
9	Cu/MgO	170	3	Ethanol	100	53.6	24
10	hcp-Co@G	220	5	H_2O	100	89.5%	52
11	Cu–Ni–Zn/HZSM-5	130	2.5	H_2O	97.4	93.4	51
12	CuCo@N–CNT	200	5	1,4-Dioxane	100	74.1	17

lyst promote the C=O bond activation of LA and lactone group of GVL, consequently resulting in a high 1,4-PDO selectivity. The catalyst support greatly affects Ru dispersion, electron structure, catalyst acidity, and hence, catalytic performance. Ru loaded on Al_2O_3–Co_3O_4 gave a 1,4-PDO yield of *ca.* 35% with a major by-product of 2-butanol at 220 °C.[33] The large number of acid sites on the Al_2O_3–Co_3O_4 support and the high reaction temperature caused serious decarboxylation of the 4-hydroxylpentanoic acid intermediate to 2-butanol.

ReO_x- and MoO_x-modified noble metal catalysts are often employed for hydrodeoxygenation of biomass,[34–36] because ReO_x and MoO_x can effectively tune the electronic structure and improve the dispersion of metal species. In addition, partially reduced ReO_x and MoO_x possess considerable numbers of oxygen vacancies that can behave as acid sites to activate the GVL intermediate. Pinel's group reported a series of heterogeneous Re-promoted noble–metal (Ru, Pd or Pt) catalysts for the hydrogenation of bio-based carboxylic acids.[37] Among these catalysts, RuRe/C gave the highest 1,4-PDO yield of 82% at 140 °C in water (entry 2, Table 1). It was found that LA was initially hydrogenated to GVL at a high rate, and then underwent ring-opening to transform into 1,4-PDO at a very slow rate. Kinetic studies corroborated that GVL ring-opening was the rate-determining step in the conversion of LA into 1,4-PDO. Another notable catalyst is Rh–MoO_x/SiO_2 (Fig. 1), which shows nearly 100% conversion with a 1,4-PDO yield of 70% at

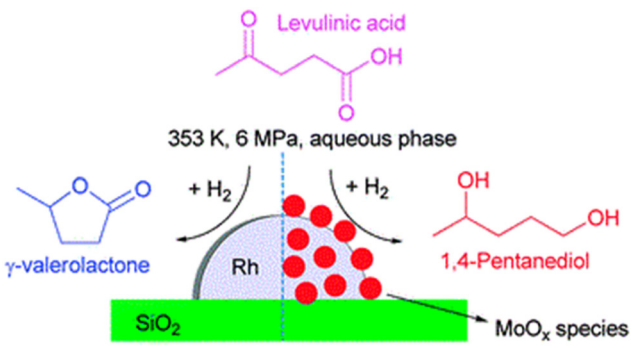

Fig. 1 LA hydrogenation to 1,4-PDO over Rh/MoO_x/SiO_2. Reproduced from ref. 38 with permission from the Royal Society of Chemistry, copyright (2014).

a low temperature of 80 °C (entry 3) due to the synergistic effect between closely contacted Rh and Mo species.[38] MoO_x enhances carboxyl acid adsorption through interaction with the lone-pair electrons of the oxygen atoms in the carbonyl group, and hence, drastically increases the carboxyl group hydrogenation rate. Recently, a MoO_x-decorated Ru/AC catalyst was prepared, and it exhibited a 1,4-PDO yield as high as 96.7% at 70 °C (entry 4).[39] In addition, its catalytic performance can be well maintained within 200 h in a continuous fixed-bed reactor. Rodiansono and co-workers found that the high catalytic performance (entry 5) of MoO_x-modified Ru/TiO_2 in LA hydrogenation to 1,4-PDO was due to the presence of Brφnsted acid sites produced by surface Mo^{6+}–OH species.[40] However, Kaneda's group assumed that the oxygen vacancies in reduced Mo species acted as Lewis acid sites to activate carbonyl moieties of GVL,[41] which highlighted the promotional role of MoO_x for Pt (entry 6). These studies show that the catalytic roles of ReO_x and MoO_x still remain under debate, which needs to be clarified by further research.

The increase of noble metal dispersion and exposure of more active sites by structural optimization are the most used strategies to improve their utilization efficiency and lower the catalyst preparation cost. Atomically dispersed metal atoms that can form strong interfacial interaction with the support achieve its utilization efficiency of 100% and high specific activity.[42–44] In comparison, metal nanoclusters provide multiple adsorption sites and adjacent metal bonds,[45,46] thus offering a variety of structural possibilities and benefiting complex biomass conversion. Li and co-workers found that single atomic-layered, low-nuclearity Pd clusters on N-doped carbon-coated SBA-15 (Pd_n/NC@SBA-15) showed excellent intrinsic activity with a turnover frequency (TOF) of 12 480 h^{-1} and a 1,4-PDO yield of >99% at 80 °C and 0.1 MPa (entry 7).[47] Kinetic studies revealed that Pd nanoclusters exhibited a much lower apparent activation energy (62.2 kJ mol^{-1}) than Pd single atoms (82.5 kJ mol^{-1}) and Pd nanoparticles (NPs) (105.2 kJ mol^{-1}). Theoretic calculations showed that the synergetic interaction between adjacent Pd atoms in layered Pd clusters facilitated the adsorption and activation of LA and GVL as a result of a substantial decline of the energy barrier of the rate-determining step for cleavage of the C1–O1 bond of GVL (0.59 eV) (Fig. 2), significantly lower than that of the C4–O1 bond (1.56 eV). In addition, Pd_n/NC@SBA-15 can be well reused for at least ten cycles and was evaluated on a larger scale (100-fold), evidencing its potential use in industrial applications.

Although a decrease of Au particle size or enhancement of Au–support interactions can significantly increase the oxidation activity, Au-based catalysts are rarely applied for

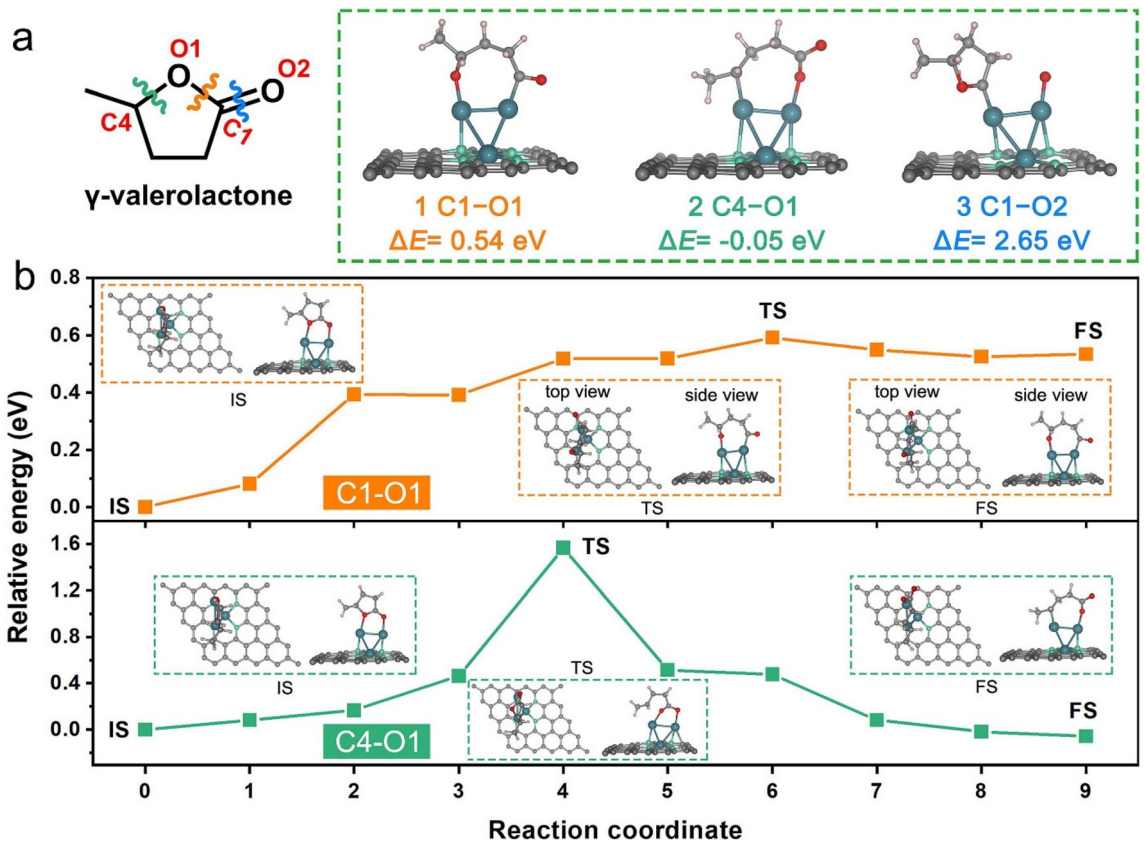

Fig. 2 (a) C–O cleavage configurations and the corresponding reaction energy on Pd_3/NC. (b) The relative energy profiles of intermediates (int) and transition states (TS) in the C–O cleavage of GVL on Pd_3/NC. IS: initial state and FS: final state. The blue, green, brown, red and white balls in the configurations represent Pd, N, C, O and H atoms, respectively. Reproduced from ref. 47 Copyright (2023), with permission from Elsevier.

biomass hydrogenation due to chemical inertness.[48] Nevertheless, Bucciol *et al.* recently demonstrated that Au/TiO_2 could convert LA into 1,4-PDO through microwave catalysis.[49] Unlike thermal catalysts, microwave catalysts can harvest the rapidly produced internal heating energy of microwaves and considerably accelerate chemical transformation, in which there are direct interactions between the electromagnetic field and reactant molecules, intermediates and/or transition states. Under microwave conditions, Au/TiO_2 gave 100% LA conversion and promoted the key ring-opening step of the GVL intermediate to 1,4-PDO.[49] In particular, 100% of 1,4-PDO yield was achieved at 200 °C under solvent-free conditions (entry 8). The ionization induced by microwaves promotes the formation of abundant H^+ species that could spillover on the surface of TiO_2. These H^+ species can rapidly react with pre-absorbed LA and GVL, thus enhancing the catalytic performance. In this case, Au acts as an active component for hydrogenation, while the TiO_2 support provides Lewis acid sites for 4-hydroxylpentanoic acid lactonization and ring-opening of GVL. Addition of water is unfavorable for the formation of 1,4-PDO due to its competitive adsorption on Lewis acid sites with the substrate of LA.

2.1.2. Non-noble metal catalysts for hydrogenation of LA to 1,4-PDO. As stated above, noble metal catalysts exhibit excellent activity and 1,4-PDO selectivity under mild conditions, but the high cost of noble metals requires development of abundant and cheap base metals, such as Cu, Co and Ni catalysts. However, base metal catalysts are much more difficult in carboxylic acid reduction than in ketone and ester.[50] Thus, many base metal catalysts, *e.g.* Cu/CN,[17] Co@CN[17] and Ni/ZSM-5,[51] are inactive for LA hydrogenation to 1,4-PDO. Hu *et al.* reported an efficient Cu/MgO catalyst derived from a layered double hydroxide precursor,[24] which showed a 1,4-PDO yield of 53.6% at 170 °C (entry 9). The basic MgO species promotes the ring-opening of GVL. Nevertheless, this catalyst suffers from serious deactivation owing to Cu NPs agglomeration.

The acidic carboxylic groups in LA molecules cause severe corrosion and sintering of non-noble metals in the reaction process. Thus, the challenge is to construct a highly active and stable base metal catalyst, particularly for metastable metal crystals. We encapsulated metastable hexagonal closed-packed (hcp) Co NPs in a few-layer thick graphene shell through pyrolysis of a metal–organic framework material of the $Co_3[Co(CN)_6]$ compound under a reductive atmosphere.[52] This hcp-Co@G catalyst could resist the corrosion of LA and, hence, showed a high 1,4-PDO yield (89.5%, entry 10) and catalytic stability. After six repeated recycles, its catalytic performance did not obviously decrease as it was well preserved by the graphene shell. It needs to be pointed out that the graphene shell contains large numbers of defective voids,[53] which allowed LA and organic molecules to freely penetrate through the graphene layer and access hcp-Co NPs.

LA has two oxygen-containing groups, the carbonyl and carboxylic groups. Compared to the carboxylic group, the carbonyl group of LA preferentially undergoes hydrogenation to produce 4-hydroxylpentanoic acid (Scheme 2). Most of the researchers reported that 4-hydroxylpentanoic acid could not be rapidly converted into 1,4-PDO,[47,52] but proceeds to lactonization to GVL. This is because reduction of the carboxylic group needs higher activation energy than lactonization. The generated GVL undergoes C–O bond cleavage (ring-opening) to form 1,4-PDO. Nevertheless, many by-products, *e.g.* 1-pentanol and 2-pentanol, are simultaneously produced due to GVL over-hydrogenolysis and 2-MTHF dehydration.

Another attractive approach to improve non-noble metal-based catalyst stability is by alloying with other metals. Formation of alloys generates new metal bonds, and hence, retards sintering and leaching during the reaction process.[54] Kim *et al.* prepared Zn-modified CuNi alloy on ZSM-5, which led to a 1,4-PDO yield of 93.4% at 130 °C in LA hydrogenation (entry 11).[51] CuNi alloy facilitates H_2 spillover, suppresses leaching of CuNi species, and thus decreases CuNi NP sintering, consequently resulting in a remarkable improvement in catalytic activity and recyclability. After five cycles, only a small decrease was detected in LA conversion and 1,4-PDO yield. In

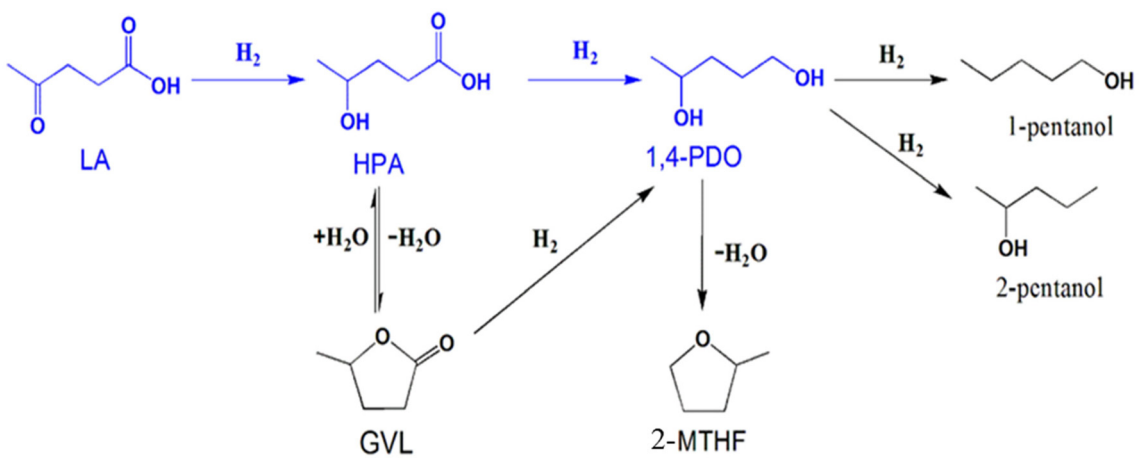

Scheme 2 Reaction pathway for LA hydrogenation to 1,4-PDO. HPA: 4-hydroxylpentanoic acid. Reproduced from ref. 52 Copyright (2019), with permission from Elsevier.

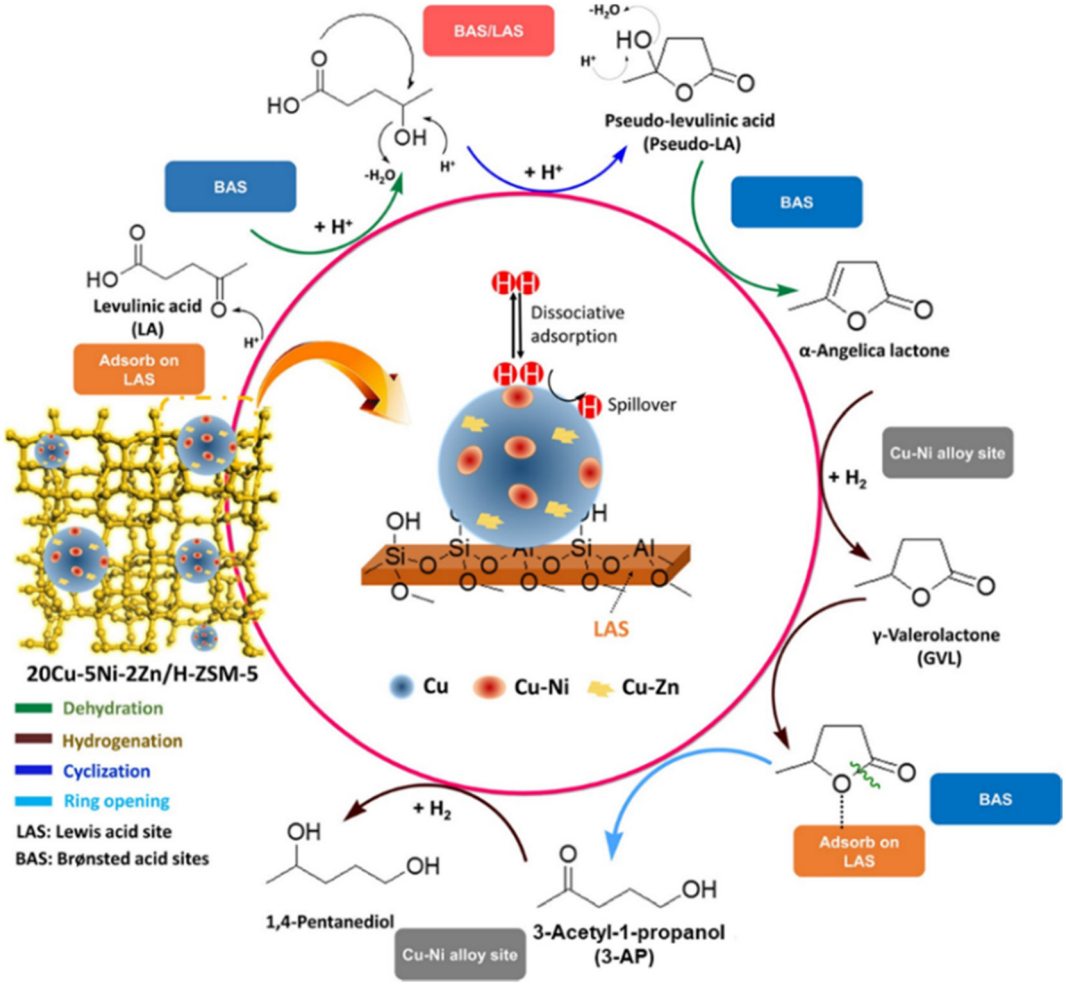

Fig. 3 Reaction pathway for LA hydrogenation to 1,4-PDO over the Cu–Ni–Zn/HZSM-5 catalyst. Reproduced from ref. 51 Copyright (2021), with permission from American Chemical Society.

the presence of strong acidic HZSM-5, a different reaction pathway was proposed for LA hydrogenation to-1,4-PDO (Fig. 3).[51] LA might initially undergo intramolecular cyclization to produce pseudo-levulinic acid, followed by dehydration on Brønsted acid sites. The formed α-angelica lactone could be rapidly hydrogenated to GVL by active H* species that were produced by dissociating H_2 on metal sites. Then, the GVL adsorbed on Lewis acid sites undergoes ring-opening through C–O bond cleavage to produce 3-acetyl-1-propanol, which is subsequently hydrogenated to 1,4-PDO on CuNi alloy. The improvement of catalytic performance is also demonstrated by the formation of CuCo alloy.[17] Compared to Co@CN (27.7%) and Cu/CN (2.0%), CuCo@N–CNTs gave a 1,4-PDO yield of 74.1% at 200 °C as a result of the electron transfer from Cu to Co (entry 12). Electron-enriched Co enhances H_2 activation, while electron-deficient Cu species generate plentiful acid sites for adsorbing the GVL intermediate and promoting its ring opening. These two factors cooperatively result in excellent catalytic performance. Moreover, 1,4-PDO selectivity only mildly decreased from 85% to 75% within five reaction runs over CuCo@N–CNTs owing to the CuCo NPs confined in N-doped carbon nanotubes.

Table 1 summarizes the representative results for the catalytic hydrogenation of LA to 1,4-PDO over various catalysts. Noble metal catalysts give a high 1,4-PDO yield at a temperature ≤140 °C due to their high intrinsic activity. High H_2 pressure is generally required to achieve superior performance except that Pd_n/NC@SBA-15 possesses very strong H_2 activation ability at ambient pressure. In contrast, base metal catalysts are generally operated at high reaction temperature. Among the used solvents, H_2O is highly promising, because biomass itself contains much water, which can save the water separation process during biomass pretreatment. It is more desirable to develop a free-solvent system to save the separation process, which needs the design of an extraordinarily active catalyst with strong acid-resistance ability.

2.2. Conversion of alkyl levulinate into 1,4-PDO

Compared to LA, alkyl levulinate does not cause catalyst component leaching and reactor corrosion as its acidic carboxyl

group has been esterified. This makes cheap non-noble catalysts a better choice for the hydrogenation of alkyl levulinate to 1,4-PDO. Ethyl levulinate and methyl levulinate as feeds are mostly used, as they can be sustainably obtained in high yields by alcoholysis of cellulose or FAL and esterification of LA with ethanol and methanol.[55–59] In EL hydrogenation, the 1,4-PDO yield reached as high as 98% at 160 °C on the ternary skeletal CuAlZn catalyst.[60] A recent research study shows that the bimetallic Cu_2Co_1/Al_2O_3 catalyst is more active and selective than monometallic Cu/Al_2O_3,[61] as it has a lower activation energy (65.1 kJ mol^{-1}) in the rate-determining step. As a result, it exhibited not only a 1,4-PDO selectivity of 93% but also high catalytic stability, as demonstrated by no obvious decrease of 1,4-PDO yield within 200 h. Introduction of CoO_x not only improves Cu dispersion and enhances H_2 activation ability due to its strong interfacial electronic interaction with Cu that modifies the Cu^0/Cu^+ ratio, evidencing the synergistic effect of Cu and electron-deficient CoO_x. Another notable catalyst is Cu/ZrO_2,[62] which yielded 39% of 1,4-PDO at 200 °C in the transfer hydrogenation of methyl levulinate with 2-propanol. The transfer hydrogenation does not require high pressure H_2, thus improving the safety of the entire process. The Cu/MgO prepared by the co-precipitation method gave a 1,4-PDO yield of 97.7% in isopropanol solvent.[63] MgO not only serves as support, but also provides abundant basic sites, thus enabling the GVL ring-opening to form 1,4-PDO. However, the H* production rate in the transfer hydrogenation process is much lower than in H_2 dissociation, which greatly lowers the reaction efficiency and retards its large-scale application. However, Cu/MgO underwent deactivation after four reaction cycles at a high Cu content owing to Cu NP agglomeration.

In the reaction process of alkyl levulinate hydrogenation to 1,4-PDO, alkyl 4-hyxoxyvalerate is another preferentially formed key intermediate, as the alkyl levulinate carbonyl group is much more easily hydrogenated than its ester group. Hu and coworkers have investigated the ethyl levulinate hydrogenation pathway on the CoMgAl catalyst by a kinetic study.[64] The carbonyl group in ethyl levulinate is firstly hydrogenated to ethyl 4-hydroxyvalerate, which is then lactonized to GVL (Scheme 3). The activation energy of the latter step is higher than that of the former one (78.0 kJ mol^{-1} *vs.* 63.5 kJ mol^{-1}). A more significant activation energy (84.0 kJ mol^{-1}) is required for the ring-opening of GVL to 1,4-PDO, showing that this elementary reaction is the rate-determining step of EL hydrogenation to 1,4-PDO.

2.3. Conversion of GVL into 1,4-PDO

Besides biomass-derived LA and ethyl levulinate, GVL is another available feedstock to synthesize 1,4-PDO. In this process, Cu-based catalysts are widely used for selective hydrogenation of esters, such as dimethyl oxalate, ethyl lactate, and γ-butyrolactone, to alcohols.[65–67] This is because Cu is efficient for C=O/C–O bond hydrogenation, but inactive for C–C bond scission. Cao *et al.* found that Cu/ZrO_2 prepared by the oxalate gel co-precipitation method shows excellent catalytic performance for the hydrogenation of GVL into 1,4-PDO.[68] The Cu/ZrO_2 with 30 wt% of Cu gave a GVL conversion of 97% and a 1,4-PDO selectivity of 99%. This catalyst even outperforms supported Ru-based catalysts under the same reaction conditions. With the inspiration of this catalyst, a variety of effective Cu-based catalysts have been fabricated for hydrogenation of GVL to 1,4-PDO. Li's group prepared a series of $Cu_x/Mg_{3-x}AlO$ catalysts based on layered double hydroxides.[69] An excellent 1,4-PDO yield was achieved on $Cu_{1.5}/Mg_{1.5}AlO$ due to the synergistic effect of well-dispersed Cu NPs and nearby appropriate surface base sites. Interestingly, a good linear relationship has been well established between the TOF value and Lewis basic site concentration (Fig. 4A). The basic sites enhance the interaction of the catalyst surface with GVL through the lone-pair electrons of the carbonyl oxygen and the π* acceptor orbital of the carbonyl carbon. The active sites of Cu^0 enable the adsorbed H_2 to dissociate into H*.

Doping of other elements into a Cu-based catalyst can stabilize and facilitate the dispersion of Cu NPs. Zhao *et al.* demonstrated the remarkable promotional effect of Zn species on the Cu/Al_2O_3 catalyst.[70] The 1,4-PDO selectivity increased from 46% on Cu/Al_2O_3 to >98% on $ZnCu/Al_2O_3$. The presence of Zn species decreases surface Lewis acid sites and suppresses the formation of by-product 2-MTHF through dehydration of 1,4-PDO (Fig. 4B). In addition, the formation of the ZnCu alloy and metallic Zn prevents metallic Cu^0 from being oxidized into Cu^{2+} species during the reaction process, and thus, improves the activity and stability. $ZnCu/Al_2O_3$ can be recycled 10 times without obvious deactivation, while GVL conversion

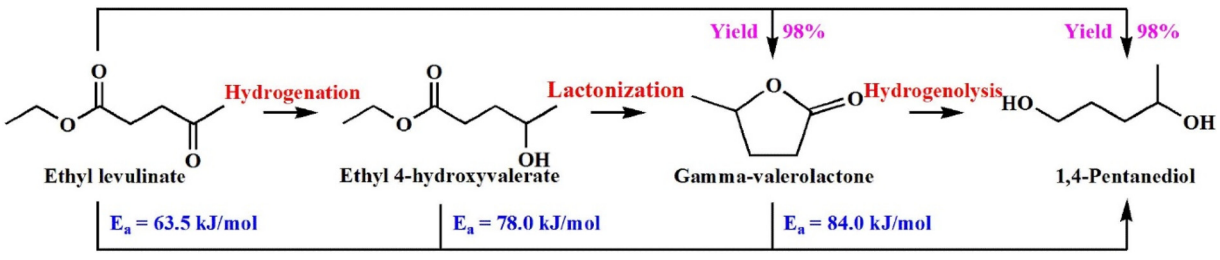

Scheme 3 Reaction pathway of ethyl levulinate hydrogenation to 1,4-PDO along with the apparent activation energies of various reaction steps. Reproduced from ref. 64 Copyright (2022), with permission from Elsevier.

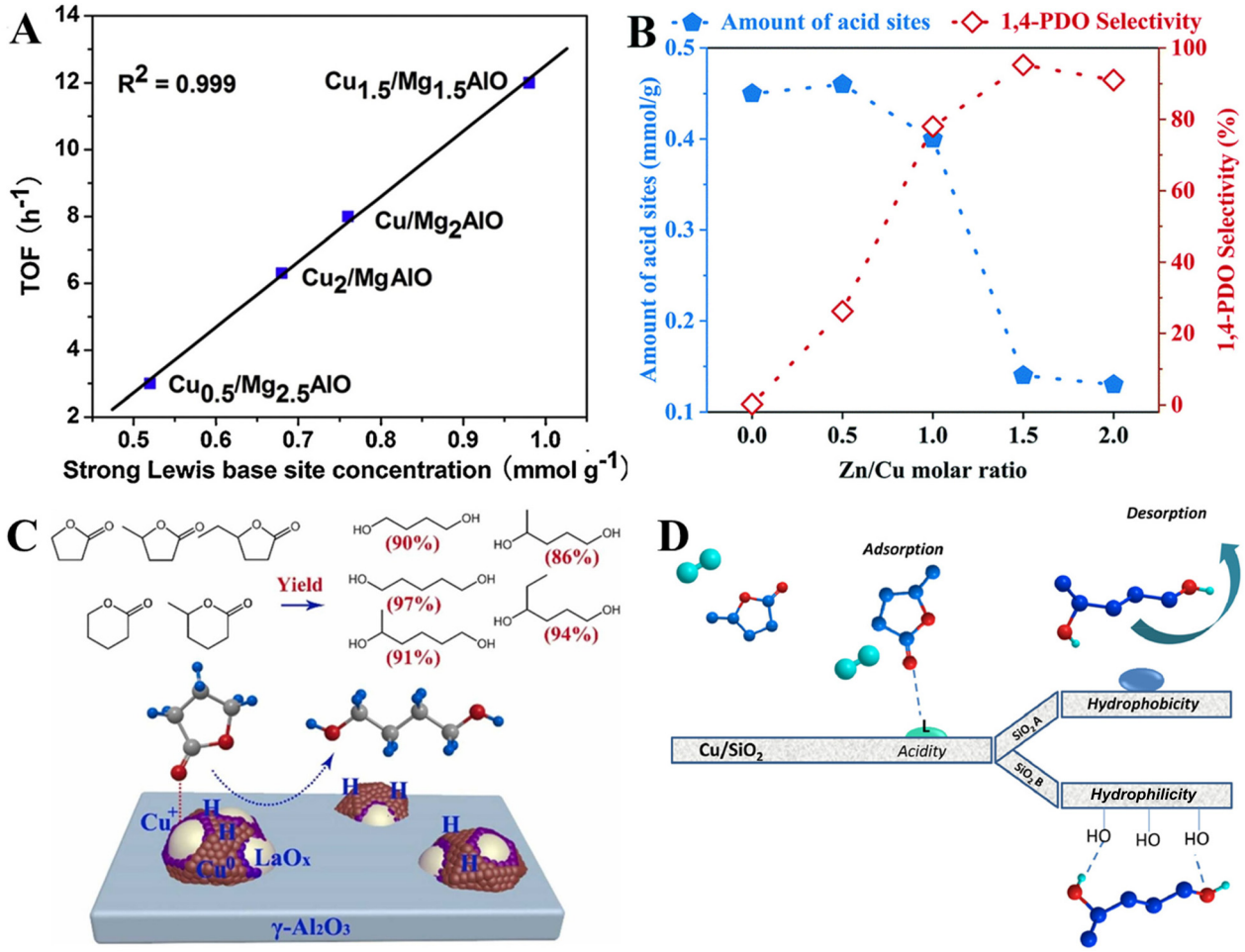

Fig. 4 (A) Linear relationship between the TOF value and the Lewis basic site concentration on different Cu/MgAlO catalysts. Reproduced from ref. 69 Copyright (2019), with permission from Elsevier. (B) Dependence of the acid site amount and 1,4-PDO selectivity on the Zn/Cu molar ratio of $ZnCu/Al_2O_3$ catalysts. Reproduced from ref. 70 with permission from the Royal Society of Chemistry, copyright (2020). (C) Catalytic results of $CuLa_x/Al_2O_3$ catalysts for conversions of various lactones into diols. Reproduced from ref. 67 Copyright (2022), with permission from Elsevier. (D) Proposed GVL adsorption and 1,4-PDO desorption mechanism on Cu/SiO_2A and Cu/SiO_2B catalysts. Reproduced from ref. 63 (2021), with permission from Elsevier.

decreased from 98% to 50% over Cu/Al_2O_3 after 5 cycles. Without ZnO doping, the active Cu species were covered by Al $(OH)_3$ owing to the formed more water originated from dehydration of 1,4-PDO. These researchers further found the promoting effect of LaO_x on Cu/Al_2O_3 catalyst,[67] which is attributed to the formation of Cu^+–LaO_x interfacial sites that enhance the GVL adsorption and activation. The $CuLa_x/Al_2O_3$ catalyst shows extensive substrate tolerance to various lactones (Fig. 4C), no matter whether they have alkyl substituents or not.

Solvent influences H_2 solubility, active metal stability, and even catalyst acidity and alkalinity. Zaccheria's team highlighted the role of the solvent in GVL hydrogenolysis to 1,4-PDO over the Cu/SiO_2 catalyst.[71] A change of the solvent from dioxane to cyclopentyl methyl ether substantially improved the 1,4-PDO selectivity due to the increase of acidic sites by 24%. The authors thought that the surface acid sites facilitated the adsorption of GVL *via* the carbonyl group (Fig. 4D), not in agreement with other reports.[47,69] This shows that the active sites for adsorption of GVL are still in debate. Acidic, basic and metallic sites are usually considered as active sites to adsorb and activate the carbonyl group of GVL, which is highly dependent on the catalyst support. In addition, it had been demonstrated that high hydrophobicity of SiO_2 support promotes 1,4-PDO desorption.

3. Conversion of furfural and its derivatives into 1,4-PDO

3.1. Conversion of furfural into 1,4-PDO

Furfural is one of a few industrially produced biomass-based platform chemicals. It is made from acid-catalyzed hemicellulose degradation. Every year, more than 200 000 tons of furfural are produced in the world.[8,72] It is interesting to convert furfural into value-added products. Early attempts by Leuck *et al.*[73] showed that furfural hydrogenation in the mixed

Table 2 Catalytic results of typical catalysts for hydrogenation of furfural to 1,4-PDO

Entry	Catalyst	Temperature (°C)	H_2 pressure (MPa)	Solvent	Conv. (%)	1,4-PDO yield (%)	Ref.
1	Ru/CMK-3	80	1	H_2O	100	90	23
2	Amberlyst-15+ Ru–FeO_x/AC	80	0.2	H_2O	100	86	74
3	PtI/Al_2O_3	100	2	Water	99.2	80.1	77
4	Ru/SC–SBA-15	140	1.5	Water	100	87	78
5	Ni–Sn alloy	160	3	Ethanol–H_2O	100	92	16
6	Cu/SiO_2	120	4	Ethanol	99.9	86.2	22

ethanol and water solvent gave a 1,4-PDO yield of 40% on RANEY® Ni catalyst. Zhang's group made significant progress in the selective production of 1,4-PDO from furfural. They reported that Ru supported on ordered mesoporous carbon (CMK-3) showed a 1,4-PDO yield of 90% in one-pot hydrogenation of furfural at 80 °C in water under pressurized H_2 and CO_2 (entry 1, Table 2).[23] As is displayed in Scheme 4, furfural is firstly hydrogenated to FAL on metallic Ru sites, and then, undergoes acid-catalyzed Piancatelli rearrangement to generate 3-acetyl-1-propanol. 3-Acetyl-1-propanol is finally hydrogenated to 1,4-PDO. The key for the formation of 1,4-PDO is to construct a weakly acidic environment that promotes the FAL Piancatelli rearrangement. The positively charged Ru species and the dissolved pressurized CO_2 in water provide necessary weakly acidic sites. Afterwards, the same group developed a continuous process with a 1,4-PDO yield of 86% by combining Amberlyst-15 and Ru–FeO_x/AC (entry 2).[74] Such a dual-component catalyst exhibited a long catalytic life of 175 h without obvious deactivation. Addition of FeO_x to Ru/AC switched the product from LA to 1,4-PDO, which is probably due to the decrease of Lewis acid sites.

As is known, to achieve excellent catalytic performance, the distribution of metal and acid sites on the catalyst need to be tailored in molecular-level proximity or formed metal–acid interface.[75,76] In addition, it has been recognized that the type of acid site plays an important role in selectivity control in furfural to 1,4-PDO. Deng *et al.* fabricated an iodine-modified Pt-based catalyst with abundant Pt–I pairs.[77] The 1,4-PDO yield reached 80.1% on this catalyst at 100 °C and 2.0 MPa H_2 (entry 3). The *in situ* hydrogen spillover-induced H^-Pt–I–H^+ pairs not only generate hydrogenation sites, but also supply Brønsted acid sites, thus enabling strong synergistic catalysis for tandem conversion of furfural to 1,4-PDO. Brønsted acid sites promote FAL ring-opening to produce the key intermediate of 3-acetyl-1-propanol. Sulfonation is an efficient method to create a large number of Brønsted acid sites. Ru NPs anchored on sulfonated carbon layer-coated SBA-15 (Ru/SC-SBA-15) exhibited a high 1,4-PDO yield of 87% under optimum conditions (entry 4).[78] The coordination of sulfonic acid groups to Ru influences Ru species electronic properties, which is beneficial for H_2 dissociation and sequential hydrogenation of the acid-hydrolyzed ring-opening intermediate. The kinetic study definitely demonstrates that the reaction preferentially occurs *via* the furfural hydrogenation to FAL, FAL to 3-acetyl-1-propanol, and finally 3-acetyl-1-propanol to 1,4-PDO in terms of obtained activation energies and rate constants.

The above-mentioned Ru and Pt-based catalysts are able to promote the conversion of furfural to 1,4-PDO under gentle conditions. However, Ru and Pt are noble and rare metals. In comparison, transition metals such as Ni and Cu are cheap

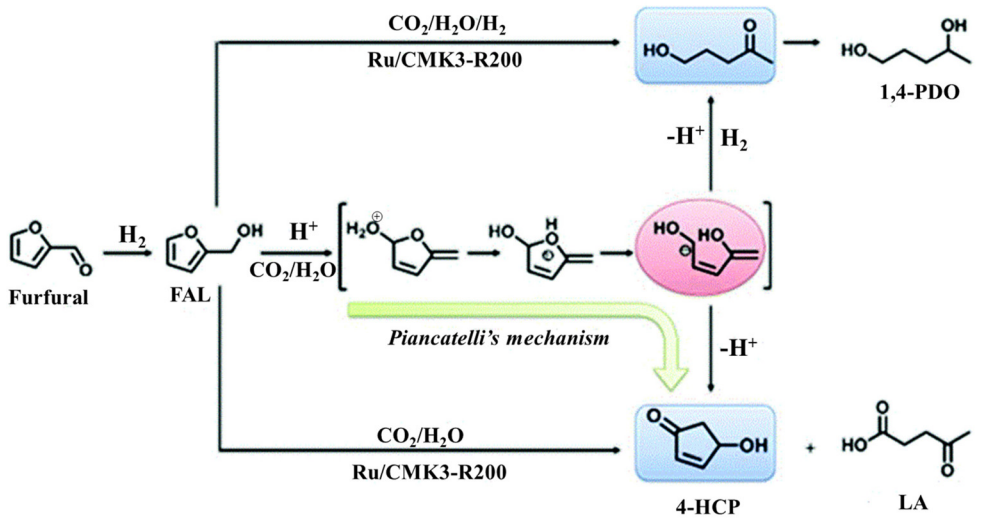

Scheme 4 Reaction pathway of furfural hydrogenation to 1,4-PDO over Ru/CMK3. 4-HCP: 4-hydroxy2-cyclopentenone. Reproduced from ref. 23 with permission from the Royal Society of Chemistry, copyright (2018).

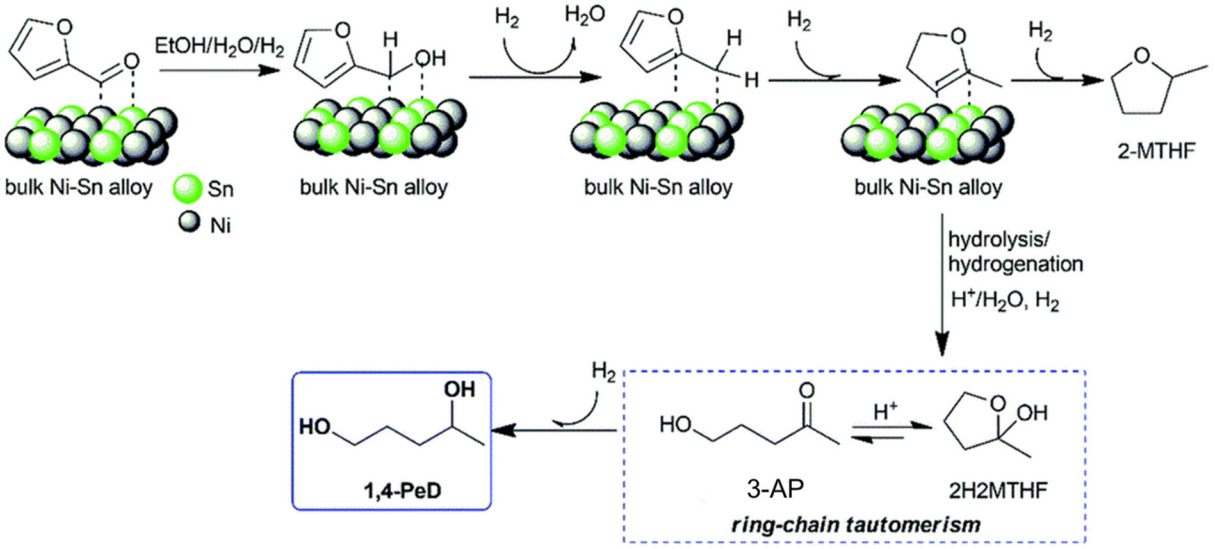

Fig. 5 Reaction mechanism for the conversion of furfural into 1,4-PDO over the bulk Ni–Sn alloy catalyst. EtOH: ethanol, 3-AP: 3-acetyl-1-propanol. 1,4-PeD: 1,4-pentanediol (1,4-PDO). Reproduced from ref. 16 with permission from the Royal Society of Chemistry, copyright (2019).

metals, which hold great potential for high catalytic performance upon elaborately structural designs and controls. Shimazu *et al.*[16] achieved a 1,4-PDO yield of 92% over the bulk Ni–Sn alloy catalyst at 160 °C and 3 MPa H_2 in an ethanol–water system (Table 2). The catalytic reaction mechanism involves in the furfural hydrogenation to FAL (Fig. 5), and protonation, dehydration and sequential hydrogenation to 2-MF. The generated 2-MF undergoes partial hydrogenation to yield 2-methyl-4,5-dihydrofuran, which is further hydrogenated to 2-hydroxy-2-methyltetrahydrofuran (2H2MTHF) on the Ni–Sn alloy surface. Upon ring-chain tautomerism *via* an equilibration reaction, 3-acetyl-1-propanol is formed and facilely hydrogenated to 1,4-PDO. Various characterization techniques confirm that Ni–SnO_x species exhibit Brønsted acidity that can promote dehydration, and the Ni_3Sn_2 alloy serves as a hydrogenation active site. These two species synergistically contribute to the hydrogenation of furfural and dehydration of FAL to key 2-MF.[79]

To date, several mechanisms have been proposed for one-pot conversion of furfural into 1,4-PDO depending on the employed solvent and catalyst. Very recently, Wang and co-workers reported a new pathway to produce 1,4-PDO with a high yield of 86.2% *via* ethanol-induced transformation of furfural (entry 6).[22] The Cu/SiO_2 catalyst derived from copper phyllosilicate enables high Cu dispersion and adequate numbers of acid sites that originated from coordinatively unsaturated Cu^{2+} and surface hydroxyl groups of copper phyllosilicate. As displayed in Fig. 6, the metallic Cu sites are capable of promoting furfural hydrogenation to FAL. This is followed by acid-catalyzed etherification between FAL and ethanol to produce 2-ethoxymethyl-furan (2-(EoM)F), which is then degraded into ethyl levulinate. Ethyl levulinate undergoes sequential hydrogenation to 1,4-PDO over Cu sites *via* formation of GVL and 3-acetyl-1-propanol intermediates.

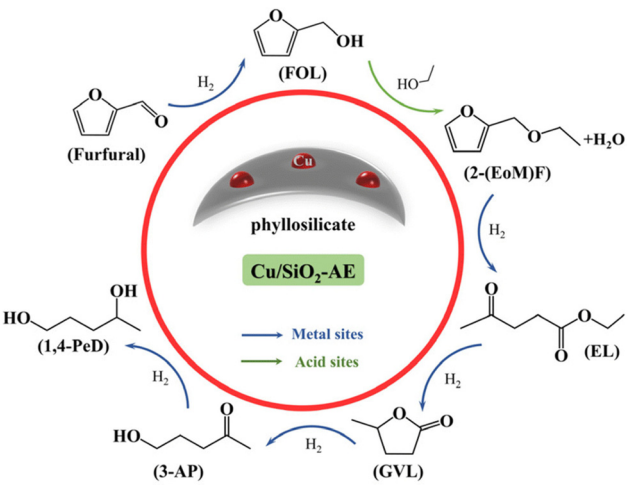

Fig. 6 Reaction pathway for the conversion of furfural into 1,4-PDO over the Cu/SiO_2–AE catalyst. 3-AP: 3-acetyl-1-propanol. EL: ethyl levulinate. Reproduced from ref. 22 with permission from the Royal Society of Chemistry, copyright (2023).

3.2. Conversion of furfural derivatives into 1,4-PDO

FAL can be facilely produced from furfural hydrogenation over Cu-based catalysts.[80,81] Direct hydrogenolysis of FAL into 1,2-PDO and 1,5-PDO has been reported with satisfactory yields under mild conditions,[82,83] but one-step conversion of FAL into 1,4-PDO is a challenge for its complex reaction pathways catalyzed by metal-acid bifunctional catalysts. At high pressure of H_2, the C=O/C=C bond of FAL is preferentially hydrogenated to generate 2-MF and 2-MTHF and the C–O bond undergoes hydrogenolysis to produce 1,2-PDO and 1,5-PDO over metal or metal–acid bifunctional catalysts, which greatly retards the formation of 1,4-PDO.[82,84] Zhu *et al.*[85] separately

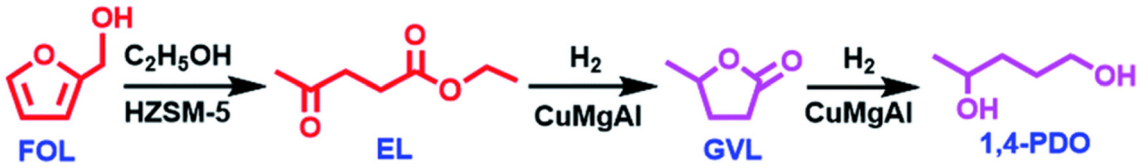

Scheme 5 Reaction pathway for the conversion of FAL into 1,4-PDO over HZSM-5 and CuMgAl catalysts. EL: ethyl levulinate. Reproduced from ref. 85 with permission from the Royal Society of Chemistry, copyright (2022).

loaded HZSM-5 and CuMgAl catalysts in the upper and lower layers of a fixed-bed reactor, respectively. HZSM-5 promoted FAL alcoholysis with ethanol to ethyl levulinate, which can be exclusively produced without the occurrence of hydrogenation by-reaction of FAL (Scheme 5). The formed ethyl levulinate is further hydrogenated to 1,4-PDO over the CuMgAl catalyst in the lower layer. Interestingly, the 1,4-PDO yield reached 94.3%. Moreover, no obvious deactivation was observed within 220 h. FAL alcoholysis was conducted in the confined acidic pores of HZSM-5 and an increased electron cloud density around Cu in the CuMgAl facilitates the activation of the EL carbonyl group.

2-MF can be sustainably obtained from furfural hydrogenation.[86,87] Thus, it is a biomass-related industrial product, and the development of processes for the conversion of 2-MF into value-added products such as 1,4-PDO is of interest. In 1947, Schniepp and co-workers made an attempt to produce 1,4-PDO from 2-MF hydrogenation in the presence of water and minor formic acid,[88] and about 50%–60% of 1,4-PDO yield was obtained. Very recently, water was demonstrated to participate in the furan ring-opening reaction in the process of 2-MF to 1,4-PDO over the PtNi bimetallic species supported on multi-walled carbon nanotubes (MWCNTs).[89] PtNi/MWCNTs gave a 1,4-PDO yield of about 69% with the aid of water. As shown in Fig. 7, 2-MF is preferentially adsorbed on the PtNi surface through the C=C bond, which is rapidly hydrogenated to 2-methyl-2,3-dihydrofuran (2-M-2,3-DIF). The $H_2{}^{18}O$ isotope labeling experiment and kinetic study results definitely confirm that water provides abundant hydroxyl groups at the C(2) position of 2-M-2,3-DIF for the formation of the key intermediate 2-methyltetrahydrofuran-2-ol (2-ME-2OL). Subsequently, intra-molecular hydrogen transfers from hydroxyl groups of the C(2) site to the O (1) group. Simultaneously, the α C–O bond is cleaved to produce 1-hydroxy-4-pentanone (1-H-4-PeO) *via* the ring-opening reaction with the H^+ attack. This process is the rate-determining step of 2-MF to 1,4-PDO. The formed 1-H-4-PeO is subsequently hydrogenated to the aimed product of 1,4-PDO. Notably, MWCNTs were superior to other supports (ZrO_2, Al_2O_3 and Nb_2O_5) in the improvement of 1,4-PDO selectivity due to the weak surface acid sites. Additionally, PtNi/MWCNTs showed high stability for at least 8 consecutive cycles, in which the 1,4-PDO yield only gently decreased from 69% to 51% because of slight Pt and Ni leaching.

2-MTHF is currently produced through 2-MF hydrogenation or furfural sequential hydrogenation.[90,91] It has been reported that 2-MTHF can be efficiently produced from LA and its

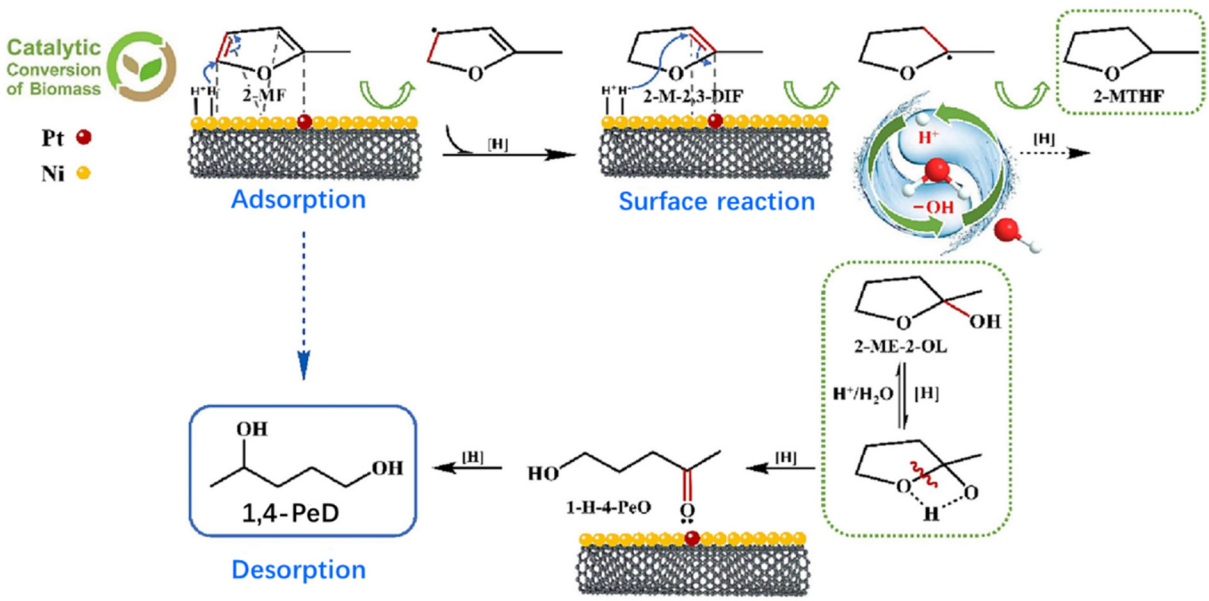

Fig. 7 Proposed reaction pathway for water-promoted hydrogenolysis of 2-MF to 1,4-PDO over the PtNi/MWNT catalyst. 1,4-PeD: 1,4-pentanediol. Reproduced from ref. 89 Copyright (2023), with permission from Elsevier.

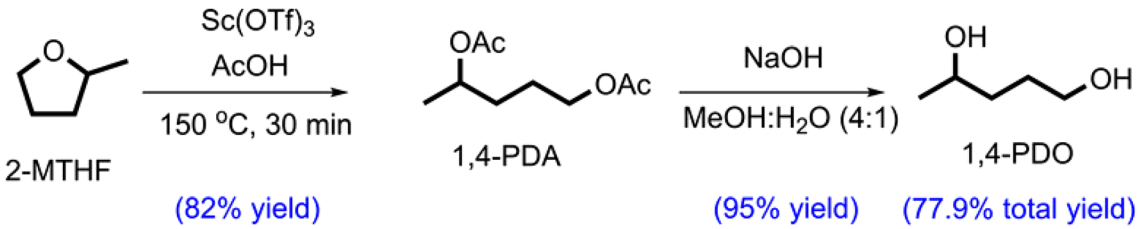

Scheme 6 Conversion of 2-MTHF into 1,4-PDO. MeOH: methanol. 1,4-PDA: 1,4-diacetoxypentane. Reproduced from ref. 95 Copyright (2018), with permission from Wiley-VCH.

derivatives of alkyl levulinate and GVL.[92–94] Fu *et al.* developed a two-step method to convert 2-MTHF into 1,4-PDO with a total yield of 77.9%,[95] as displayed in Scheme 6. In the presence of acetic acid (AcOH), 2-MTHF was converted into 1,4-diacetoxypentane with a yield of 82% on the $Sc(OTf)_3$ catalyst. Once the residual AcOH was separated from the reactor, the formed 1,4-diacetoxypentane was facilely transformed into 1,4-PDO *via* saponification when adding NaOH solution.

The industrial production of LA and its derivatives are facing many challenges from the hydrolysis/alcoholysis of cellulose. The purification of LA from water solution needs high energy consumption. Compared to LA, furfural and its derivatives have been commercially produced from hemicellulose, which has formed a very complete industrial chain. However, the abundant furfural residue and the strongly corrosive sulfuric acid process bring about severe environmental pollution. Thus, furfural has much cheaper price than LA, but shows relatively low greenness. Additionally, the acidic LA usually corrodes the catalyst and leads to the leaching of active species. However, the synthesis of 1,4-PDO from furfural requires to undergo complex tandem reactions and forms humins in water, resulting in a relatively low 1,4-PDO yield.

4. Current challenges and future prospects for 1,4-PDO production from biomass

Regardless of these great advances on the production of 1,4-PDO from biomass, many challenges should be faced, which has retarded large-scale commercial applications. (1) Although the catalytic conversion LA or furfural and their derivatives achieve high yields of 1,4-PDO under mild conditions, most of the catalytic reactions and processes are performed in batch reactors with low feed concentrations. These non-continuous processes have low production efficiency, bear strong labor load, and require high H_2 pressure. Additionally, the used catalysts unavoidably need to separate with reaction products, which can lose partial catalysts and likely raises operation costs. (2) Most of processes employ relatively rare and expensive noble metal catalysts in order to achieve good performance and improve the hydrothermal stability during high temperature and pressure environment. Particularly, the most used Ru element occupies just 0.00004 parts per million in Earth's crust. (3) Water is a green and low-price solvent that is naturally involved in biomass. Thus, water is an unavoidable and promising solvent for 1,4-PDO production. However, the use of water can lead to the formation of humins, particularly for the conversion of furan compounds, which can seriously affect the carbon balance and greatly enhance the separation cost. The hydrothermal condition and strong acid of LA in aqueous solution result in serious sintering and leaching of the metal catalyst. Moreover, the role of water on the catalyst structure and reaction mechanism has not been thoroughly investigated. (4) The production of 1,4-PDO from either LA or furfural involves several individual metal and acid-catalyzed reactions, and therefore the synergistic effect between metal and acid sites is crucial for enhancing the production rate of 1,4-PDO. The currently used catalysts don't consider the proximity of metal and acid sites, which remarkably affects the diffusion of reaction intermediates and reaction rate owing to spatially separated metal NPs and acid sites. (5) Previous research studies predominantly focused on the catalytic performance (activity, selectivity and stability) and reaction condition optimization, while the reaction mechanism has been rarely investigated in detail. The complex cascade reaction process as well as harsh reaction conditions greatly enhance the difficulties to probe catalyst structure evolution during the reaction process by *in situ* or *operando* characterization techniques.

Biomass is an abundant renewable carbon source with carbon neutrality. Conversion of biomass-based LA, furfural and their derivatives is an effective way to decline the reliance on fossil resources. To achieve this goal, many challenging and long-standing issues should be resolved by tailoring an advanced catalyst and deep recognition of the reaction mechanism. Future research is emphasized in following directions that could bring about significant progress in 1,4-PDO production. (1) Continuous flow or slurry bed reactors can significantly enhance the production efficiency of 1,4-PDO, which is beneficial for large-scale application. Measurement of accurate and meaningful kinetic parameters enables the design of an optimal reactor. Meanwhile, it is necessary to probe the best reaction route in the thermodynamic state space. Tracking a fluid element on its way through the reactor, manipulating the flux profiles and minimizing the residence time are also essential prerequisites for reactor optimization.[96] (2) Further efforts

are needed to decline the catalyst cost that is still a main limitation for commercial production of 1,4-PDO. A single atom catalyst offers the maximum atom efficiency and 100% metal dispersion.[42,97] Thus, this is an ideal strategy to create single metal atoms anchored on supports, which can remarkably reduce the cost of using expensive noble metals. Additionally, the development of Earth-abundant alloy catalysts can save the costs and construct a robust structure *via* the formation of relatively strong alloy bonds to stabilize metal atoms against dissolution. Alloying can also tune the electronic structure and decrease the C═O group adsorption energy of LA and furfural, which has been shown to enhance catalytic activity.[53] (3) The use of a high substrate concentration can obviously decline the production costs. It is indispensable to exploit efficient separation methods such as using a two-phase system with immiscible organics or a deep eutectic solvent, which can simplify difficult and energy-intensive isolation procedures. Additionally, fabrication of water-resistant catalysts is an effective method to synthesize 1,4-PDO in water. Many catalysts with core–shell, alloy, or confinement structures are endowed with good hydrothermal stability.[53,98] Alternatively, active metal leaching by acidic LA can be circumvented by selectively covering hydrophobic support. It is also necessary to probe the role of water in catalyst leaching and the reaction mechanism by advanced techniques such as *operando* Raman spectroscopy and D_2O-isotope labeling. (4) To achieve catalytic benefits from bifunctional active sites outperforms those from a single optimal active site, because the cooperation between different types of active sites can remarkably enhance the 1,4-PDO yield for cascade conversion of LA/furfural.[99] To improve the proximity of metal and acid sites for maximizing their synergy effect, it is essential to tailor the distribution of catalytic sites and control the catalyst structure with the formation of a metal–acid interface. Encapsulation of metal NPs into the pores of zeolites can fabricate the geometrically closest metal NPs with acid sites, which greatly shortens the diffusion distance of LA/furfural molecules to access the metal–acid active sites.[100,101] Construction of well-separated metal–MoO_x (or ReO_x) pair catalysts can form abundant metal–acid interfaces,[99] in which pairs of active sites work synergistically to promote 1,4-PDO production from LA or furfural. Additionally, the geometry structure of the metal–MoO_x interface, adaptive reconstruction and inter-site communication are crucial for dual catalytic behavior during the reaction process.[99] (5) Powerful *operando* characterization techniques or density functional theory (DFT) calculations tools are applied to elucidate the cascade reaction mechanism of LA or furfural to 1,4-PDO. Operando liquid nuclear magnetic and X-ray absorption spectra that are adaptable to high-temperature and high-pressure liquid media can be used to trap key intermediates (GVL and 3-acetyl-1-propanol) and obtain kinetic data. DFT calculation based on machine learning molecular dynamics simulation has been used as a general and automated way to visualize and understand the surface reaction mechanism referring to each elementary reaction[29,102] The metal–acid dual site structure directly involves in the catalytic cycle by adsorbing and activating LA/furfural as well as intermediates. The reaction process including the transition state configuration and the energy change during every step can be traced and quantitatively calculated at the atomic level. (6) The harness of biomass *via* emerging photo-/electrocatalytic approaches may foster the development of green H_2 production. Combining furfural or LA hydrogenation at the anode and the hydrogen evolution reaction at the cathode in a biomass electrolysis or photo-reforming reactor perhaps affords an appealing strategy for producing 1,4-PDO with low environmental costs and carbon footprint.[103]

5. Conclusions

This review summarizes the conversion of biomass-derived LA and furfural as well as their derivatives into valuable 1,4-PDO. The used catalysts, structure–performance correlation, reaction pathway and mechanism have been well discussed in detail. Comparatively, the reaction pathway of LA-to-1,4-PDO has been well identified, in which LA initially hydrogenates to 4-hydroxylpentanoic acid, which proceeds with lactonization to GVL, and it undergoes ring-opening to 1,4-PDO. However, the reaction pathway of furfural to 1,4-PDO is still a debate, which highly depends on the used catalyst and reaction solvent. Conversion of LA suffers from catalyst deactivation owing to the acidic properties of LA, and thus there are emerging ReO_x/MoO_x modified noble metal catalysts or non-noble metals with special structures such as core–shell or alloy. Conversion of furfural to 1,4-PDO involves a complex and variable cascade reaction, which greatly enhances the difficulty in understanding the reaction mechanism.

Although 1,4-PDO synthesis from biomass has achieved notable advances, particularly for obtaining a high yield of 1,4-PDO, a variety of challenges, such as process development, catalysts, solvent, active site distribution and reaction mechanism, should be faced ahead of the industrial production. We provide various strategies for improving the possibility of large-scale application of 1,4-PDO and driving future research toward the development of profitable biorefinery operations for highly-efficient conversion of biomass into 1,4-PDO. In summary, it is of great significance to exploit an economically viable technique for expanding the biomass conversion roadmap of 1,4-PDO for achieving both carbon neutrality and environmental protection, which will offer potential opportunities for multidisciplinary experts involving material scientists, chemists, engineers and economists.

Conflicts of interest

There are no conflicts to declare.

Acknowledgements

We greatly acknowledge the financial support by the National Natural Science Foundation of China (22278416), the

Fundamental Research Program of Shanxi Province for Excellent Young Scholars (20210302122015), and ICC CAS (SCJC-DT-2023-02).

References

1 Y. Jing, Y. Guo, Q. Xia, X. Liu and Y. Wang, *Chem*, 2019, **5**, 2520–2546.
2 M. He, Y. Sun and B. Han, *Angew. Chem., Int. Ed.*, 2022, **61**, e202112835.
3 L. T. Mika, E. Cséfalvay and Á. Németh, *Chem. Rev.*, 2018, **118**, 505–613.
4 M. M. Abu-Omar, K. Barta, G. T. Beckham, J. S. Luterbacher, J. Ralph, R. Rinaldi, Y. Román-Leshkov, J. S. M. Samec, B. F. Sels and F. Wang, *Energy Environ. Sci.*, 2021, **14**, 262–292.
5 Y. Liao, S.-F. Koelewijn, G. V. D. Bossche, J. V. Aelst, S. V. D. Bosch, T. Renders, K. Navare, T. Nicolaï, K. V. Aelst, M. Maesen, H. Matsushima, J. M. Thevelein, K. V. Acker, B. Lagrain, D. Verboekend and B. F. Sels, *Science*, 2020, **367**, 1385–1390.
6 Y. Liu, N. Deak, Z. Wang, H. Yu, L. Hameleers, E. Jurak, P. J. Deuss and K. Barta, *Nat. Commun.*, 2021, **12**, 5424.
7 A. J. Ragauskas, G. T. Beckham, M. J. Biddy, R. Chandra, F. Chen, M. F. Davis, B. H. Davison, R. A. Dixon, P. Gilna, M. Keller, P. Langan, A. K. Naskar, J. N. Saddler, T. J. Tschaplinski, G. A. Tuskan and C. E. Wyman, *Science*, 2014, **344**, 1246843.
8 R. Mariscal, P. Maireles-Torres, M. Ojeda, I. Sadaba and M. L. Granados, *Energy Environ. Sci.*, 2016, **9**, 1144–1189.
9 J.-P. Lange, E. van der Heide, J. van Buijtenen and R. Price, *ChemSusChem*, 2012, **5**, 150–166.
10 D. Di Menno Di Bucchianico, Y. Wang, J.-C. Buvat, Y. Pan, V. Casson Moreno and S. Leveneur, *Green Chem.*, 2022, **24**, 614–646.
11 Z. Yu, X. Lu, J. Xiong, X. Li, H. Bai and N. Ji, *ChemSusChem*, 2020, **13**, 2916–2930.
12 A. A. Rosatella, S. P. Simeonov, R. F. M. Frade and C. A. M. Afonso, *Green Chem.*, 2011, **13**, 754–793.
13 Q. Wang, J. Feng, L. Zheng, B. Wang, R. Bi, Y. He, H. Liu and D. Li, *ACS Catal.*, 2020, **10**, 1353–1365.
14 B. Katryniok, H. Kimura, E. Skrzynska, J.-S. Girardon, P. Fongarland, M. Capron, R. Ducoulombier, N. Mimura, S. Paul and F. Dumeignil, *Green Chem.*, 2011, **13**, 1960–1979.
15 Y.-K. Hong, D.-W. Lee, H.-J. Eom and K.-Y. Lee, *Appl. Catal., B*, 2014, **150–151**, 438–445.
16 Rodiansono, M. Dewi Astuti, T. Hara, N. Ichikuni and S. Shimazu, *Green Chem.*, 2019, **21**, 2307–2315.
17 Y. Wei, J. Lu, S. Zhang, C. Wu, X. Nong, J. Li, C.-L. Liu and W.-S. Dong, *Chem. Commun.*, 2023, **59**, 2477–2480.
18 B. M. Stadler, A. Brandt, A. Kux, H. Beck and J. G. de Vries, *ChemSusChem*, 2020, **13**, 556–563.
19 E. Benisvy-Aharonovicha, A. Zandanya, A. Saadya, Y. Kinel-Tahanb, Y. Yehoshuab and A. Gedanken, *Bioresour. Technol. Rep.*, 2020, **11**, 100514.
20 T. Sugimura, H. Iguchi, R. Tsuchida, A. Tai, N. Nishiyama and T. Hakushi, *Tetrahedron: Asymmetry*, 1998, **9**, 1007–1013.
21 T. Sugimura, H. Yamada, S. Inoue and A. Tai, *Tetrahedron: Asymmetry*, 1997, **8**, 649–655.
22 Y. Zheng, J. Zang, Q. Zhang, X. Wu, S. Qiu, Q. Meng and T. Wang, *Green Chem.*, 2023, **25**, 1128–1136.
23 F. Liu, Q. Liu, J. Xu, L. Li, Y.-T. Cui, R. Lang, L. Li, Y. Su, S. Miao, H. Sun, B. Qiao, A. Wang, F. Jérôme and T. Zhang, *Green Chem.*, 2018, **20**, 1770–1776.
24 Y. Shao, K. Sun, Q. Li, Q. Liu, S. Zhang, Q. Liu, G. Hu and X. Hu, *Green Chem.*, 2019, **21**, 4499–4511.
25 C. Michel and P. Gallezot, *ACS Catal.*, 2015, **5**, 4130–4132.
26 S. Shao, Y. Yang, K. Sun, S. Yang, A. Li, F. Yang, X. Luo, S. Hao and Y. Ke, *ACS Catal.*, 2021, **11**, 12146–12158.
27 W. Cao, W. Luo, H. Ge, Y. Su, A. Wang and T. Zhang, *Green Chem.*, 2017, **19**, 2201–2211.
28 K. Zhang, Q. Meng, H. Wu, T. Yuan, S. Han, J. Zhai, B. Zheng, C. Xu, W. Wu, M. He and B. Han, *Green Chem.*, 2021, **23**, 1621–1627.
29 X. Gao, S. Zhu, M. Dong, J. Wang and W. Fan, *J. Catal.*, 2020, **389**, 60–70.
30 J. Tan, J. Cui, T. Deng, X. Cui, G. Ding, Y. Zhu and Y. Li, *ChemCatChem*, 2015, **7**, 508–512.
31 V. K. Velisoju, G. B. Peddakasu, N. Gutta, V. Boosa, M. Kandula, K. V. R. Chary and V. Akula, *J. Phys. Chem. C*, 2018, **122**, 19670–19677.
32 J. Lv, Z. Rong, L. Sun, C. Liu, A.-H. Lu, Y. Wang and J. Qu, *Catal. Sci. Technol.*, 2018, **8**, 975–979.
33 R. Wang, L. Chen, X. Zhang, Q. Zhang, Y. Li, C. Wang and L. Ma, *RSC Adv.*, 2018, **8**, 40989–40995.
34 M. Tamura, R. Tamura, Y. Takeda, Y. Nakagawa and K. Tomishige, *Chem. – Eur. J.*, 2015, **21**, 3097–3107.
35 Z. Wang, G. Li, X. Liu, Y. Huang, A. Wang, W. Chu, X. Wang and N. Li, *Catal. Commun.*, 2014, **43**, 38–41.
36 Y. Takeda, T. Shoji, H. Watanabe, M. Tamura, Y. Nakagawa, K. Okumura and K. Tomishige, *ChemSusChem*, 2015, **8**, 1170–1178.
37 L. Corbel-Demailly, B.-K. Ly, D.-P. Minh, B. Tapin, C. Especel, F. Epron, A. Cabiac, E. Guillon, M. Besson and C. Pinel, *ChemSusChem*, 2013, **6**, 2388–2395.
38 M. Li, G. Li, N. Li, A. Wang, W. Dong, X. Wang and Y. Cong, *Chem. Commun.*, 2014, **50**, 1414–1416.
39 J. Cui, J. Tan, Y. Zhu and F. Cheng, *ChemSusChem*, 2018, **11**, 1316–1320.
40 Rodiansono, A. S. Azzahra, H. P. Dewi, I. B. Adilina and K. C. Sembiring, *Catal. Sci. Technol.*, 2023, **13**, 4466–4476.
41 T. Mizugaki, Y. Nagatsu, K. Togo, Z. Maeno, T. Mitsudome, K. Jitsukawa and K. Kaneda, *Green Chem.*, 2015, **17**, 5136–5139.
42 P. Liu, Y. Zhao, R. Qin, S. Mo, G. Chen, L. Gu, D. M. Chevrier, P. Zhang, Q. Guo, D. Zang, B. Wu, G. Fu and N. Zheng, *Science*, 2016, **352**, 797–800.
43 L. Lin, W. Zhou, R. Gao, S. Yao, X. Zhang, W. Xu, S. Zheng, Z. Jiang, Q. Yu, Y.-W. Li, C. Shi, X.-D. Wen and D. Ma, *Nature*, 2017, **544**, 80–83.

44 A. J. Therrien, A. J. R. Hensley, M. D. Marcinkowski, R. Zhang, F. R. Lucci, B. Coughlin, A. C. Schilling, J.-S. Mc Ewen and E. C. H. Sykes, *Nat. Catal.*, 2018, **1**, 192–198.
45 J. Zhang, M. Wang, Z. Gao, X. Qin, Y. Xu, Z. Wang, W. Zhou and D. Ma, *J. Am. Chem. Soc.*, 2022, **144**, 5108–5115.
46 X. Zhang, M. Zhang, Y. Deng, M. Xu, L. Artiglia, W. Wen, R. Gao, B. Chen, S. Yao, X. Zhang, M. Peng, J. Yan, A. Li, Z. Jiang, X. Gao, S. Cao, C. Yang, A. J. Kropf, J. Shi, J. Xie, M. Bi, J. A. van Bokhoven, Y.-W. Li, X. Wen, M. Flytzani-Stephanopoulos, C. Shi, W. Zhou and D. Ma, *Nature*, 2021, **589**, 396–401.
47 X. Lu, T. Luo, M. Zhang, J. Hugh Horton, Q. Wu, W. Wu, M. Qiao, Y. Wang and Z. Li, *Chem. Eng. J.*, 2023, **464**, 142647.
48 W. Zhan, Q. He, X. Liu, Y. Guo, Y. Wang, L. Wang, Y. Guo, A. Y. Borisevich, J. Zhang, G. Lu and S. Dai, *J. Am. Chem. Soc.*, 2016, **138**, 16130–16139.
49 F. Bucciol, S. Tabasso, G. Grillo, F. Menegazzo, M. Signoretto, M. Manzoli and G. Cravotto, *J. Catal.*, 2019, **380**, 267–277.
50 T. J. Korstanje, J. Ivar van der Vlugt, C. J. Elsevier and B. de Bruin, *Science*, 2015, **350**, 298–302.
51 N. Karanwal, M. G. Sibi, M. K. Khan, A. A. Myint, B. Chan Ryu, J. W. Kang and J. Kim, *ACS Catal.*, 2021, **11**, 2846–2864.
52 X. Gao, S. Zhu, M. Dong and W. Fan, *J. Catal.*, 2021, **399**, 201–211.
53 S. Zhu, H. Liu, S. Wang, X. Gao, P. Wang, J. Wang and W. Fan, *Appl. Catal., B*, 2021, **284**, 119698.
54 Z. W. Seh, J. Kibsgaard, C. F. Dickens, I. Chorkendorff, J. K. Nørskov and T. F. Jaramillo, *Science*, 2017, 355.
55 K.-I. Tominaga, A. Mori, Y. Fukushima, S. Shimada and K. Sato, *Green Chem.*, 2011, **13**, 810–812.
56 D. Zhao, P. Prinsen, Y. Wang, W. Ouyang, F. Delbecq, C. Len and R. Luque, *ACS Sustainable Chem. Eng.*, 2018, **6**, 6901–6909.
57 J.-P. Lange, W. D. van de Graaf and R. J. Haan, *ChemSusChem*, 2009, **2**, 437–441.
58 H. Tian, Y. Shao, C. Liang, Q. Xu, L. Zhang, S. Zhang, S. Liu and X. Hu, *Renewable Energy*, 2020, **162**, 1576–1586.
59 S. Zhu, C. Chen, Y. Xue, J. Wu, J. Wang and W. Fan, *ChemCatChem*, 2014, **6**, 3080–3083.
60 D. Ren, X. Wan, F. Jin, Z. Song, Y. Liu and Z. Huo, *Green Chem.*, 2016, **18**, 5999–6003.
61 J. Wu, G. Gao, P. Sun, X. Long and F. Li, *ACS Catal.*, 2017, **7**, 7890–7901.
62 Y. Yang, X. Xu, W. Zou, H. Yue, G. Tian and S. Feng, *Catal. Commun.*, 2016, **76**, 50–53.
63 M. Fan, Y. Shao, K. Sun, Q. Li, S. Zhang, Y. Wang, J. Xiang, S. Hu, S. Wang and X. Hu, *Mol. Catal.*, 2021, **510**, 111680.
64 Y. Shao, S. Ba, K. Sun, G. Gao, M. Fan, J. Wang, H. Fan, L. Zhang and X. Hu, *Chem. Eng. J.*, 2022, **429**, 132433.
65 Y. Zhu, Y. Zhu, G. Ding, S. Zhu, H. Zheng and Y. Li, *Appl. Catal., A*, 2013, **468**, 296–304.
66 L. Huang, Y. Zhu, H. Zheng, M. Du and Y. Li, *Appl. Catal., A*, 2008, **349**, 204–211.
67 Q. Xu, C. Wang, Z. Shang, C. Zhang, X. Wang, Q. Liu, L. Dang, Y. Liu and F. Zhao, *Appl. Catal., B*, 2022, **317**, 121689.
68 X.-L. Du, Q.-Y. Bi, Y.-M. Liu, Y. Cao, H.-Y. He and K.-N. Fan, *Green Chem.*, 2012, **14**, 935–939.
69 J. Wu, G. Gao, Y. Li, P. Sun, J. Wang and F. Li, *Appl. Catal., B*, 2019, **245**, 251–261.
70 Q. Liu, Z. Zhao, M. Arai, C. Zhang, K. Liu, R. Shi, P. Wu, Z. Wang, W. Lin, H. Cheng and F. Zhao, *Catal. Sci. Technol.*, 2020, **10**, 4412–4423.
71 D. Cavuoto, N. Ravasio, N. Scotti, A. Gervasini, S. Campisi, M. Marelli, G. Cappelletti and F. Zaccheria, *Mol. Catal.*, 2021, **516**, 111936.
72 S. Zhu, Y. Cen, J. Guo, J. Chai, J. Wang and W. Fan, *Green Chem.*, 2016, **18**, 5667–5675.
73 G. J. Leuck, J. Pokorny and F. N. Peters, *US Pat.*, 2097493, Nov. 2, 1937.
74 Q. Liu, B. Qiao, F. Liu, L. Zhang, Y. Su, A. Wang and T. Zhang, *Green Chem.*, 2020, **22**, 3532–3538.
75 H. J. Cho, D. Kim, S. Li, D. Su, D. Ma and B. Xu, *ACS Catal.*, 2020, **10**, 3340–3348.
76 J. He, Z. Wu, Q. Gu, Y. Liu, S. Chu, S. Chen, Y. Zhang, B. Yang, T. Chen, A. Wang, B. M. Weckhuysen, T. Zhang and W. Luo, *Angew. Chem., Int. Ed.*, 2021, **60**, 23713–23721.
77 L. Zhang, X. Li, J. Wang, Z. Zeng, W. Yang, S. Deng and Q. Deng, *AIChE J.*, 2023, **69**, e17996.
78 K. Cui, W. Qian, Z. Shao, X. Zhao, H. Gong, X. Wei, J. Wang, M. Chen, X. Cao and Z. Hou, *Catal. Lett.*, 2021, **151**, 2513–2526.
79 Rodiansono, A. S. Azzahra, P. R. Ansyah, S. Husain and S. Shimazu, *RSC Adv.*, 2023, **13**, 21171–21181.
80 P. Cao, L. Lin, H. Qi, R. Chen, Z. Wu, N. Li, T. Zhang and W. Luo, *ACS Catal.*, 2021, **11**, 10246–10256.
81 K. Chen, J.-L. Ling and C.-D. Wu, *Angew. Chem., Int. Ed.*, 2020, **59**, 1925–1931.
82 B. Zhang, Y. Zhu, G. Ding, H. Zheng and Y. Li, *Green Chem.*, 2012, **14**, 3402–3409.
83 R. Ma, X.-P. Wu, T. Tong, Z.-J. Shao, Y. Wang, X. Liu, Q. Xia and X.-Q. Gong, *ACS Catal.*, 2017, **7**, 333–337.
84 Y. Zhu, W. Zhao, J. Zhang, Z. An, X. Ma, Z. Zhang, Y. Jiang, L. Zheng, X. Shu, H. Song, X. Xiang and J. He, *ACS Catal.*, 2020, **10**, 8032–8041.
85 H. Wang, Y. Wang, L. Huang, A. Geng, F. Yi, Y. Zhu and Y. Li, *Sustainable Energy Fuels*, 2022, **6**, 2449–2461.
86 Y. Deng, R. Gao, L. Lin, T. Liu, X.-D. Wen, S. Wang and D. Ma, *J. Am. Chem. Soc.*, 2018, **140**, 14481–14489.
87 S. Iqbal, X. Liu, O. F. Aldosari, P. J. Miedziak, J. K. Edwards, G. L. Brett, A. Akram, G. M. King, T. E. Davies, D. J. Morgan, D. K. Knight and G. J. Hutchings, *Catal. Sci. Technol.*, 2014, **4**, 2280–2286.
88 L. E. Schniepp, H. H. Geller and R. W. V. Korff, *J. Am. Chem. Soc.*, 1947, **69**, 672–674.

89 M. Wu, T. Wang, W. Li, Q. Zhang, B. Zhang, K. Chen, S. Peng, G. Li, J. Huang, Q. Wang and C. Wang, *Chem. Eng. J.*, 2023, **461**, 141944.
90 P. Liu, L. Sun, X. Jia, C. Zhang, W. Zhang, Y. Song, H. Wang and C. Li, *Mol. Catal.*, 2020, **490**, 110951.
91 F. Dong, Y. Zhu, G. Ding, J. Cui, X. Li and Y. Li, *ChemSusChem*, 2015, **8**, 1534–1537.
92 A. Phanopoulos, A. J. P. White, N. J. Long and P. W. Miller, *ACS Catal.*, 2015, **5**, 2500–2512.
93 Y.-B. Huang, A.-F. Liu, Q. Zhang, K.-M. Li, W. B. Porterfield, L.-C. Li and F. Wang, *ACS Sustainable Chem. Eng.*, 2020, **8**, 11477–11490.
94 Z. Xie, B. Chen, H. Wu, M. Liu, H. Liu, J. Zhang, G. Yang and B. Han, *Green Chem.*, 2019, **21**, 606–613.
95 K. Zhang, X.-L. Li, S.-Y. Chen, H.-J. Xu, J. Deng and Y. Fu, *ChemSusChem*, 2018, **11**, 726–734.
96 A. Peschel, H. Freund and K. Sundmacher, *Ind. Eng. Chem. Res.*, 2010, **49**, 10535–10548.
97 L.-N. Chen, K.-P. Hou, Y.-S. Liu, Z.-Y. Qi, Q. Zheng, Y.-H. Lu, J.-Y. Chen, J.-L. Chen, C.-W. Pao, S.-B. Wang, Y.-B. Li, S.-H. Xie, F.-D. Liu, D. Prendergast, L. E. Klebanoff, V. Stavila, M. D. Allendorf, J. Guo, L.-S. Zheng, J. Su and G. A. Somorjai, *J. Am. Chem. Soc.*, 2019, **141**, 17995–17999.
98 N. Wang, Q. Sun, R. Bai, X. Li, G. Guo and J. Yu, *J. Am. Chem. Soc.*, 2016, **138**, 7484–7487.
99 I. Ro, J. Qi, S. Lee, M. Xu, X. Yan, Z. Xie, G. Zakem, A. Morales, J. G. Chen, X. Pan, D. G. Vlachos, S. Caratzoulas and P. Christopher, *Nature*, 2022, **609**, 287–292.
100 Z. Jin, X. Yi, L. Wang, S. Xu, C. Wang, Q. Wu, L. Wang, A. Zheng and F.-S. Xiao, *Appl. Catal., B*, 2019, **254**, 560–568.
101 J. Yang, Y. He, J. He, Y. Liu, H. Geng, S. Chen, L. Lin, M. Liu, T. Chen, Q. Jiang, B. M. Weckhuysen, W. Luo and Z. Wu, *ACS Catal.*, 2022, **12**, 1847–1856.
102 Z. Zeng, F. Wodaczek, K. Liu, F. Stein, J. Hutter, J. Chen and B. Cheng, *Nat. Commun.*, 2023, **14**, 6131.
103 H. Luo, J. Barrio, N. Sunny, A. Li, L. Steier, N. Shah, I. E. L. Stephens and M. Titirici, *Adv. Energy Mater.*, 2021, **11**, 2101180.